Computation of the solutions of the Fokker-Planck equation for one and two DOF systems

Franziska Schmidt, Claude-Henri Lamarque

Computation of the solutions of the Fokker-Planck equation for one and two DOF systems

F. Schmidt *, C.-H. Lamarque

Laboratoire GéoMatériaux, Ecole Nationale Des Travaux Publics de l'Etat, Vaulx-en-Velin, France

Abstract

Uncertainty in structures may come from unknowns in the modelisation and in the properties of the materials, from variability with time, external noise... This leads to uncertainty in the dynamic response. Moreover, the consequences are issues in safety, reliability, efficiency... of the structure. So an issue is the gain of information on the response of the system taking into account the uncertainties.

If the forcing or the uncertainty can be modelled through a white noise, the Fokker-Planck (or Kolmogorov forward) equation exists. It is a partial differential linear equation with unknown $p(X,t)$, where $p(X,t)$ is the probability density function of the state X at time t.

In this article, we solve this equation using the finite differencesmethod, for one and two DOF systems. The numerical solutions obrtained are proved to be nearly correct.

Key words: Discrete nonlinear mechanical systems, Fokker-Planck equation, energy pumping.

1 Introduction

Today there is growing concern about uncertainties in dynamic structures. In fact, these uncertainties may come from unknowns in the properties of the structure or in the sollicitations, and this leads to uncertainties in the response.

* Corresponding author.
Email addresses: schmidt@entpe.fr (F. Schmidt), lamarque@entpe.fr (C.-H. Lamarque).

There exists two kinds of techniques to solve this problem : the possibilistic ([6,23,1,18,17,14]) and the probabilistic approaches ([24,22]).

The first ones just use an assessment of the interval of variation of the fluctuating parameters, sollicitations,... The second ones also assume a probability density function for the properties that are uncertain.

An other possibility may be the existence of an uncertainty whose origin,and thus their variations, are unknown.

Here we study the Fokker-Planck equation of some dynamical systems, which is a partial differential equation with unknown $p(X,t)$, where $p(X,t)$ is the probability of the state X at time t. For this, these systems are assumed to undergo a white noise, which can represent random forces or parameters.

In Section 2 we apply the theory of the Fokker-Planck equation to one-degree-of-freedom systems. We propose a simulation whose accuracy is checked. Afterwards we try to meet some deterministic phenomenons in this probabilistic study. In Section 3, we deal with a two-degree-of-freedom system leading to energy pumping. Finally, in a last part we will conclude by displaying the pros and the cons of this method.

2 Computation for 1 DOF systems

An analytical solution of the Fokker-Planck equation is known only in some specific cases, see e.g. [21,26,11]. That's why to solve the Fokker-Planck equation of the dynamical systems we study, we chose the method of finite differences, coupled with the time-splitting method ([19,29,31]).

Let us consider the equation of a non-linear oscillator :

$$\begin{aligned} \dot{y}_1 &= y_2 \ , \\ \dot{y}_2 + g(y_1, y_2, t) &= f(t) \ . \end{aligned} \tag{1}$$

$f\left(t\right)$ is a random gaussian white noise such as :

$$< f\left(t\right) >= 0, < f\left(t_1\right) f\left(t_2\right) >= \frac{W_0}{2} \delta\left(t_1 - t_2\right) \ .$$

This noise can stand for the forcing the system undergoes, but also for uncertainties.
The Fokker-Planck equation of this system is given by ([21]) :

$$\frac{W_0}{4}\frac{\partial^2 p}{\partial y_2^2} - \frac{\partial}{\partial y_1}(y_2 p) + \frac{\partial}{\partial y_2}\{g(y_1, y_2)p\} = \frac{\partial p}{\partial t} \ . \tag{2}$$

We split the operator in three parts :

$$\frac{\partial p}{\partial t} = \mathcal{L}^* p = \mathcal{L}_1 p + \mathcal{L}_2 p + \mathcal{L}_3 p \tag{3}$$

$$\text{with :} \quad \begin{cases} \mathcal{L}_1 p = \dfrac{\partial}{\partial y_1}\left[-y_2 p\right] \ , \\ \mathcal{L}_2 p = \dfrac{\partial}{\partial y_2}\left[g(y_1, y_2)p\right] \ , \\ \mathcal{L}_3 p = \dfrac{\partial^2}{\partial y_2^2}\left[\dfrac{W_0}{4}p\right] \ . \end{cases} \tag{4}$$

So in the general case, the algorithm can be written :

$$\begin{cases} p^{n+1/3} = \mathcal{U}_1(p^n) \ , \\ p^{n+2/3} = \mathcal{U}_2(p^{n+1/3}) \ , \\ p^{n+1} = \mathcal{U}_3(p^{n+2/3}) \ , \end{cases} \tag{5}$$

where $\mathcal{U}_1, \mathcal{U}_2, \mathcal{U}_3$ are finite difference schemes discretizing respectively $\mathcal{L}_1$, $\mathcal{L}_2$, $\mathcal{L}_3$. They may be implicit Euler, explicit Euler, Cranck-Nicholson..., see next section. p^n, $p^{n+1/3}$, ... are vectors of discretized states at points of the finite difference grid at discrete times t_n, $t_{n+1/3}$, ... respectively.

2.1 Test of different numerical schemes and comparison with the exact solution

An analytical solution of equation (2) for a Duffing-type oscillator ($g(y_1, y_2) = ay_2 + by_1 + cy_1^3$) is known if and only if the non-linearity coefficient is null ($c = 0$). This solution can be found for example in [21]. We use this case to test the accuracy of our numerical solution.

We set the numerical values of the parameters according to [30] : $N = 40$, $L_1 = L_2 = 4$, $a = 2.1$, $k = 1$ et $W_0 = 3.2$, where $2N + 1$ is the number of nodes per direction, L_1 and L_2 are the length of the domain of study in each direction. The initial condition for the algorithm is the exact solution at time $t = 0.95s$ coming from $(x_0, y_0) = (0, 0)$.

First we compare the errors of different schemes. For this, we use two representations of the error : $||e||_1 = \sqrt{\frac{1}{(2N+1)(2N+1)} \sum_{i,j} \left(p_{i,j}^{exact} - p_{i,j}^{num}\right)^2}$ and $||e||_2 = \left(\frac{\sum_{i,j} \left(p_{i,j}^{exact} - p_{i,j}^{num}\right)^2}{\sum_{i,j} \left(p_{i,j}^{exact}\right)^2} \right)^{1/2}$.

We tried purely implicit schemes, upwind differencing, explicit, staggered leapfrog and Cranck-Nicholson.

By comparing the errors after 310 time-steps ($t = 0.973896s$), it can be seen that in every case, a good choice may be the implicit Euler scheme because it is always stable and its error is small. On graph 1, the errors of the numerical solution obtained with different combinations of schemes are drawn :

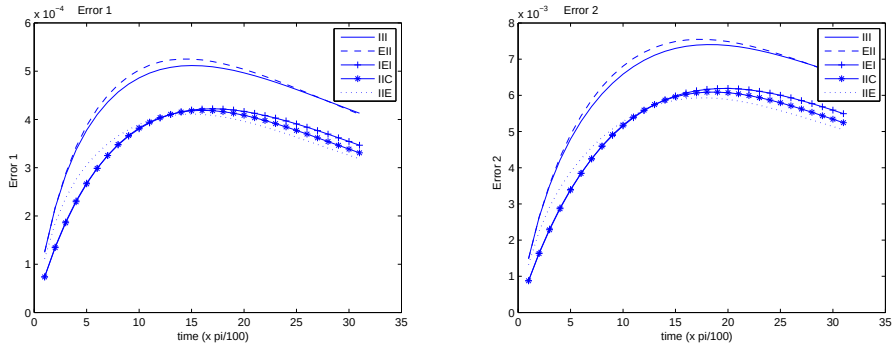

Figure 1. Norms 1 and 2 of the error for different combinations of schemes. "I" stands for "implicit", "E" for "explicit", "C" for "Cranck-Niholson". So "III" means the combination of schemes "implicit+implicit+implicit".

Moreover, the calculation times of all these combinations are similar.

We also check the accuracy of the solution obtained by splitting the operator only in two parts (so with just one intermediate timestep), as in ([29], [31]). If we compare this way of programming with the combination of three schemes "implicit + implicit + implicit", the simulation which splits the operator with two intermediate time-steps is much more accurate and faster.

Finally, we also checked the case where the conditions at the limits of the domain of study are not null, but equal to ϵ, with $\epsilon << 1$. The best results are obtained with ϵ small. In fact, they would be obtained with limit conditions equal to the exact solution at the limits of the domain of study. So, for a domain of study sufficiently vast to contain all the phenomenons of the motion, null limit conditions are the best choice.

2.2 Test of different numerical values of the parameters and comparison with the exact solution

According to what has been said just before, we now use only purely implicit schemes.

While comparing the exact solution with our numerical result, we see that the error increases quite quickly until $t = \frac{\pi}{5} = 0.6283s$ (see figure 2). The maximum which is reached is $||e||_1 = 0.00051180$ and $||e||_2 = 0.006057$. After that, the norms of the errors decrease slowly. The time of calculation (CPU) is $4.8484375.10^2$ until $t = \frac{6\pi}{5}$.
The maximum of error occurs at the states where the peak of the probability

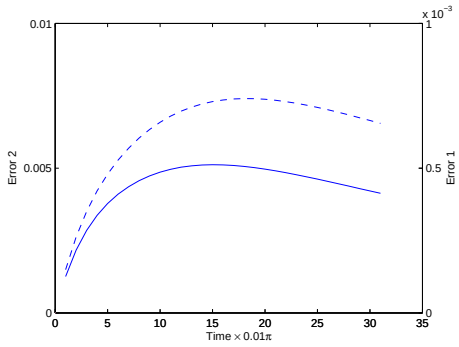

Figure 2. Evolution of the norms of the error along time. The dotted line represents error 2, whereas the full one stands for error 1.

density function is located. This means that his location and his base are correct, but his height is slightly smaller in the numerical solution. But this loss of height is acceptable : between 2% and 10%. This decrease in the height of the peak is due to losses of energy in the domain of study, outside the peak, where the density of probability calculated numerically is gently bigger than it should. As the integral of the density of probability all over the domain of study is normed to 1, this makes the peak be less tall.

We now test different other numerical values for the parameters. Then we compare the numerical solution with the exact one, that is to say the analytical one.
We give the errors at $t = \frac{31\pi}{100}s = 0.973896s$ (see table 1) :

This can be commented pertinently :

- The simulations with a too small diffusion coefficient or a too limited domain of study are unacceptable. In the first case, the reason is that because of the value of W_0, the matrix given by the Euler implicit scheme may be

Numerical value of the parameters	Norm 1	Norm 2	Comments
Default : $N = 40$, $\Delta t = \frac{\pi}{2000}$, $L_1 = L_2 = 4$, $W_0 = 3.2$	$4.1307.10^{-4}$	0.006547	
$N = 40$, $\Delta t = \frac{\pi}{500}$, $L_1 = L_2 = 4$, $W_0 = 3.2$	$7.36253.10^{-4}$	0.0117223	
$N = 40$, $\Delta t = \frac{\pi}{1000}$, $L_1 = L_2 = 4$, $W_0 = 3.2$	$9.17225.10^{-4}$	0.01459	
$N = 20$, $\Delta t = \frac{\pi}{2000}$, $L_1 = L_2 = 4$, $W_0 = 3.2$	0.00431	0.06928	
$N = 80$, $\Delta t = \frac{\pi}{2000}$, $L_1 = L_2 = 4$, $W_0 = 3.2$	$6.4155.10^{-4}$	0.01010	
$N = 160$, $\Delta t = \frac{\pi}{2000}$, $L_1 = L_2 = 4$, $W_0 = 3.2$	$8.8087.10^{-4}$	0.01383	
$N = 40$, $\Delta t = \frac{\pi}{2000}$, $L_1 = L_2 = 2$, $W_0 = 3.2$	0.13214	0.529303	
$N = 40$, $\Delta t = \frac{\pi}{2000}$, $L_1 = L_2 = 4$, $W_0 = 0.32$	0.1315411	0.6593023	Loss of height of the peak, increase of the probability outside the peak
$N = 40$, $\Delta t = \frac{\pi}{2000}$, $L_1 = L_2 = 4$, $W_0 = 0.032$	0.6598393	0.998853	Disappearance of the peak, density equal everywhere

Table 1
Norms of the error while changing numerical values of the parameters.

ill-conditioned. Then, because of the density of probability compelled to be null at the limits of the domain of study, this last one must be sufficiently large to contain all the dynamical phenomenons of the system.

- Otherwise the errors are very small. Moreover, the numerical values of the parameters choosen in [29] and [31] give the best result : this is the case because they may have been choosen in order to work with the best conditioned system.

To conclude this section, we claim that our numerical scheme gives good results. But a previous deterministic calculation may be usefull, in order to determinate the best domain of study (just large enough) and the best parameters for the simulation (time step, space steps..) in order to work with

the best-conditioned matrices.

2.3 Comparison with known 1 DOF systems

Following [12], we study this dynamical system :

$$\begin{cases} \dot{x} = y \\ \dot{y} = -dy + x - x^3 + a\cos(\tau) \\ \dot{\tau} = 1 \end{cases} \tag{6}$$

The numerical values of the parameters are set : $d = 0.15$, $a = 0.3$, $W_0 = 0.01$, $N = 200$, $L_1 = 4$, $L_2 = 4$, $\Delta t = 0.2\pi$. Results of [12] are found again. By representing the Poincaré section, the two equilibrium points at $(x = \pm 1, y = 0)$ and the strange attractor can be seen (figure 3).

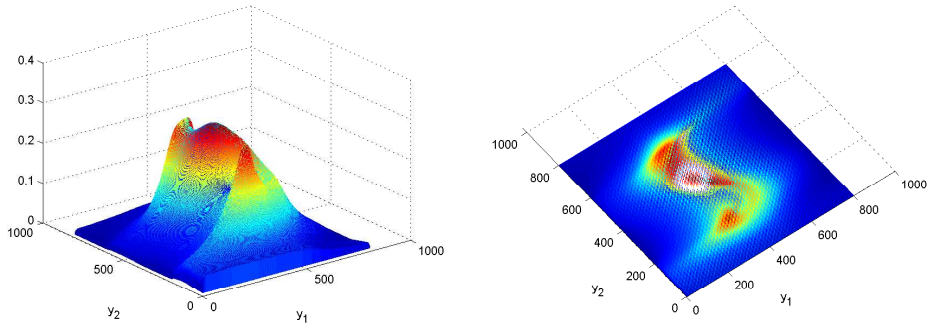

Figure 3. Poincaré section of the Fokker-Planck probability density for the Duffing–like oscillator (6). Here $t = 90T$, where T is the period of the forcing.

We study the parametric system of [16] :

$$\ddot{u} + \delta\dot{u} + \left(w_0^2 + \gamma\cos(wt)\right)u + \alpha u^2 + \beta u^3 = f(t) \quad , \tag{7}$$

$f(t)$ is a white noise of diffusion coefficient W_0.

For the numerical simulation, we choose the parameters of ([16], page 116) : $\delta = 0.9$, $\gamma = 0.9$, $w_0 = 1$, $w = 1.895$, $\alpha = 1$, $\beta = 1$. If the initial condition choosen is a dirac located in the zone of attraction of the limit cycle of period $\dfrac{4\pi}{w}$, the Poincaré section is just a peak (see figures 4) located upon the fixed point corresponding to the periodic solution.

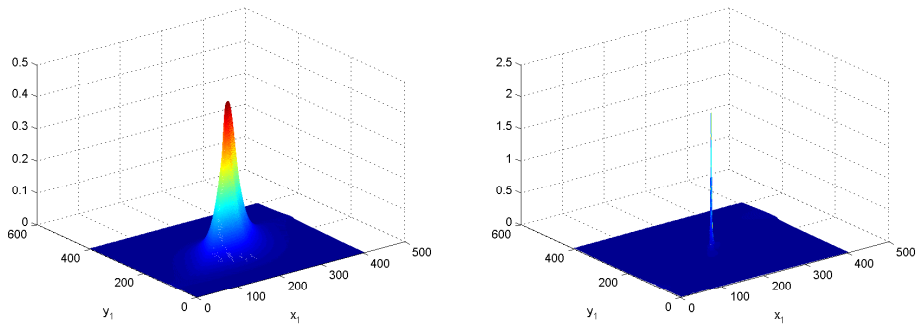

Figure 4. Poincaré section of the system (7), with $\delta = 0.9$, $\gamma = 0.9$, $w_0 = 1$, $w = 1.895$, $\alpha = 1$, $\beta = 1$ and an initial condition located in the zone of attraction of the limit cycle of period $\dfrac{4\pi}{w}$. This section is given for $t = T$ (on the left) and $t = 40T$ (on the right).

To observe the other zones of attraction (those of the attractors with two or four strips), it is necessary to choose a convenient initial condition (see figures 5). Our results are coherent with complicated deterministic ones ([16]) : the probability density plotted via Poincaré section of period $\dfrac{2\pi}{w}$ of figures 5 is spread upon attarctors.

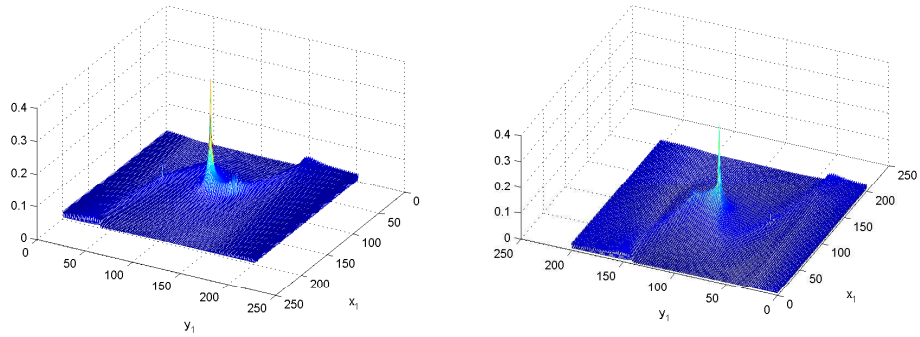

Figure 5. Poincaré section of the system (7), with $\delta = 0.9$, $\gamma = 0.9$, $w_0 = 1$, $w = 1.895$, $\alpha = 1$, $\beta = 1$ and an initial condition located in the zone of attraction of the strange attractor with two strips.

2.4 Study of a quasi non-smooth system

The Fokker-Planck equation is difficult to obtain for non-smooth systems. We do not know mathematical results leading to a correct equation with additional boundary conditions corresponding to "obstacles" created by the associated "free boundary" problem : e.g. for impact problems, the displacement can be bounded, so the space variables in the Fokker-Palnck equation have

a boundary. But in a purely non-smooth system, one has to add boundary conditions to solve the Fokker-Planck equation.

That's why we study the following quasi non-smooth system :

$$m\ddot{x} + a\dot{x} + kx + \alpha\sigma(\dot{x}) = r\sin(wt) + f(t) \ , \tag{8}$$

where :

- $f(t)$ is a white noise whose diffusion coefficient is $\dfrac{W_0}{2}$.
- $\tilde{\sigma}(x)$ is the following function :

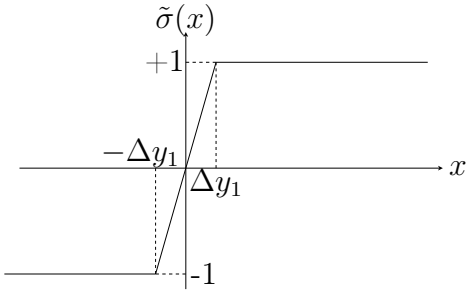

$$\tilde{\sigma}(x) = \begin{cases} -1 & \text{si} \quad x < -\Delta y_1 \\ \dfrac{x}{\Delta y_1} & \text{si} \quad x \in [-\Delta y_1, \Delta y_1] \\ 1 & \text{si} \quad x > \Delta y_1 \ . \end{cases}$$

Figure 6. Graph of the function as it is used in the simulation.

The probabilistic results are similar to the deterministic ones, seen for example in [13] : for small times, the phase portrait has the shape of the line segment $\left[-\dfrac{\alpha}{k}, \dfrac{\alpha}{k}\right]$. After that, it looses its shape and rotate of quite 90°. Its form is that of an S, whose ends go on curving until looking like a snail.

So with an amplitude of the sollicitation small, the evolution of the Fokker-Planck probability density function is the same : first, it has the shape of a line segment until a limit time (quite 0.3π here), then it bends. In the end, it winds around itself until having the shape of a snail (or a rose). For long times, this spiral spreads more and more.

This behavior can be summed up by figure 7 (page 10).

For long times, the ends of the S bends until having the shape of a snail (figures 8 and 9, page 11), in agreement with deterministic mechanism.

3 Computation for 2 DOF systems

The term "energy pumping" means the transfer of energy from one mean structure to an auxiliary secondary one ([7,8,28,5,25]). Here the mean structure

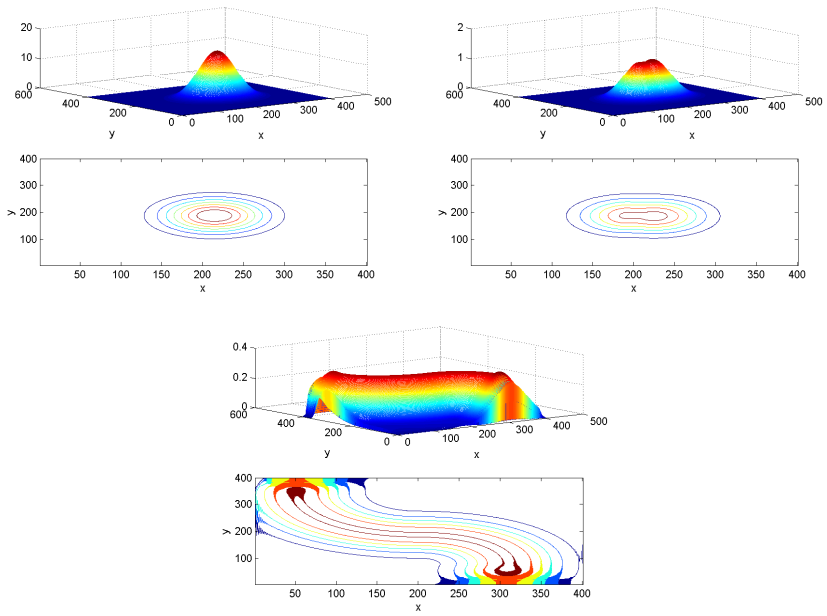

Figure 7. Fokker-Planck probability density function of the dynamical system described by the equation (8) with $m = 1$, $a = 0.03$, $k = 1.0$, $\alpha = 1.0$, $r = 0.1$, $w = 0.9$. For this computation, we set the timestep $\Delta t = 0.001\pi$, the domain of study $[-1.5, 1.5] \times [-1.5, 1.5]$, the number of nodes in the mesh per direction is $N = 200$, the diffusion coefficient of the white noise is $W_0 = 0.001$. The initial condition is a gaussian centered in $(0.1, 0.1)$. The times that are represented here are $t = 0$, $t = 30\Delta t$ and $t = 530\Delta t$. Thus we observe that the density function, that initially is a gaussian, takes the shape of a line segment from $-\frac{\alpha}{k}$ to $+\frac{\alpha}{k}$, which curves rapidly.

is linear, whereas the other one is a non-linear, Duffing-like oscillator. We consider the following system :

$$\begin{cases} M\ddot{x} + \lambda_1 \dot{x} + k_1 x + \gamma(x - y) = f_1(t) \ , \\ m\ddot{y} + \lambda_s \dot{y} + Cy^3 + \gamma(y - x) = f_2(t) \ , \end{cases} \tag{9}$$

with these initial conditions :

$$\begin{cases} x(0) = y(0) = \dot{y}(0) = 0 \ , \\ \dot{x}(0) = \sqrt{2h} \ , \end{cases} \tag{10}$$

and $f_1(t)$ et $f_2(t)$ are two white non-correlated noises whose diffusion coefficients are respectively W_{01} et W_{02}, so :

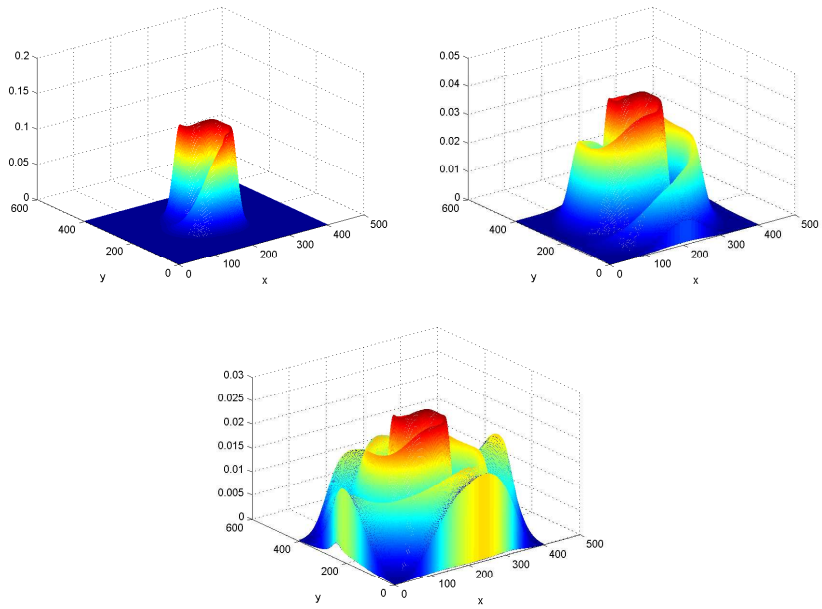

Figure 8. Fokker-Planck probability density function of the same dynamical system as in graph (7). The times that are pictured are $10\times0.01\pi$, $20\times0.01\pi$ and $30\times0.01\pi$. So for important observation times, the line segment bends at its ends until having the shape of an "S". After that, it winds around itself until resembling a snail. But this phenomenon does not stop, it means that this density function goes on winding around, spreading more and more in space. So the domain study should be more and more vast as time increases.

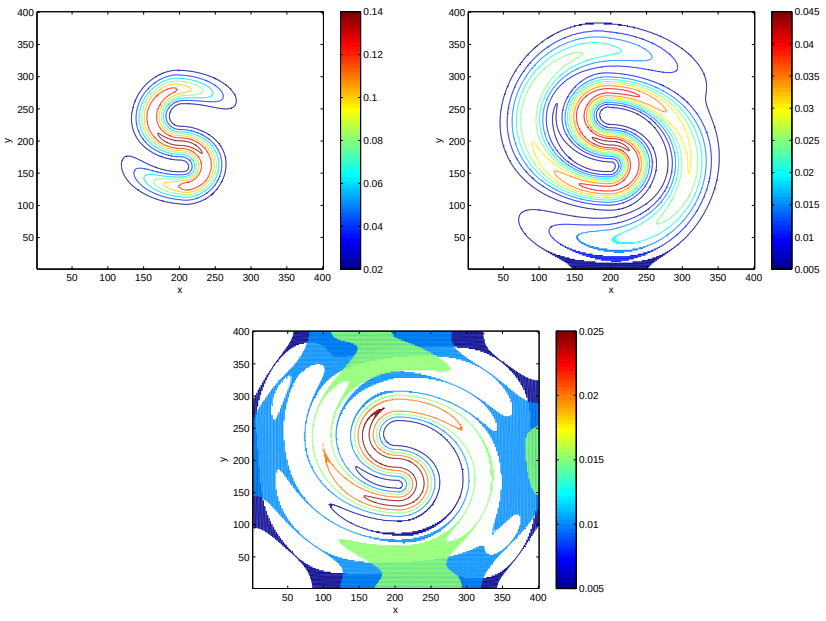

Figure 9. Contours of the Fokker-Planck probability density function of picture (7). Chronologically the times are $10 \times 0.01\pi$, $20 \times 0.01\pi$ and $30 \times 0.01\pi$ (the sames as before, on figure 7).

$$\begin{cases} < f_1(t) > = 0 \ , \\ < f_2(t) > = 0 \ , \\ \forall (i,j) \in \{1,2\}^2 \ , \ < f_i(t_k) . f_j(t_l) > = \dfrac{W_{0i}}{2} \delta_{ij} \delta(t_k - t_l) \ . \end{cases} \tag{11}$$

In the deterministic case ($f_1(t) = f_2(t) = 0$), this energy pumping can be noticed through the positions of the two oscillators along time or the variation of their energy (see figure 10) :

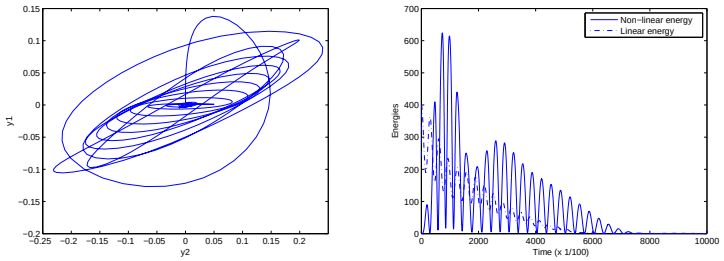

(a) Position of oscillator 2 versus position of oscillator 1.

(b) Energy of the two oscillators along time.

Figure 10. Existence of energy pumping in system (9) with : $M = 1$, $\lambda_1 = 0.01$, $k_1 = 1$, $\gamma = 0.04$, $m = 0.05$, $\lambda_s = 0.01$, $C = 1$, $h = 0.1$ ([8]). At $t = 0$, only oscillator 1 is in motion (line quite vertical). Then the range of the oscillations of oscillator 1 increases until reaching a maximum (about 0.12), the oscillator 2 begins to oscillate. Energy is transferred, the oscillations y_2 are more and more important (curves more and more slopped). After that, the oscillator 2 is the only one to oscillate until reaching the complete rest. So when the linear energy reaches a threshold, the non-linear energy increases. After that, both decrease until being null.

The Fokker-Planck equation for the system (9) is :

$$\begin{aligned} \frac{\partial p}{\partial t} = & -y_2 \frac{\partial p}{\partial y_1} + \frac{\partial}{\partial y_2} \left[\left(\lambda_1 y_2 + k_1 y_1 + \gamma (y_1 - y_3) \right) p \right] + \frac{W_{01}}{4} \frac{\partial^2 p}{\partial y_2^2} \\ & -y_4 \frac{\partial p}{\partial y_3} + \frac{\partial}{\partial y_4} \left[\left(\lambda_s y_4 + C y_3^3 + \gamma (y_3 - y_1) \right) p \right] + \frac{W_{02}}{4} \frac{\partial^2 p}{\partial y_4^2} \ . \end{aligned} \tag{12}$$

We split this equation in six parts :

$$\frac{\partial p}{\partial t} = \mathcal{L}_1 p + \mathcal{L}_2 p + \mathcal{L}_3 p + \mathcal{L}_4 p + \mathcal{L}_5 p + \mathcal{L}_6 p \ , \tag{13}$$

with : $\mathcal{L}_1 = -y_2 \dfrac{\partial}{\partial y_1}$, $\mathcal{L}_2 = \dfrac{\partial}{\partial y_2} \left[\lambda_1 y_2 + k_1 y_1 + \gamma (y_1 - y_3) \right]$, $\mathcal{L}_3 = \dfrac{W_{01}}{2} \dfrac{\partial^2}{\partial y_2^2}$,

$$\mathcal{L}_4 = -y_4 \frac{\partial}{\partial y_3},$$
$$\mathcal{L}_5 = \frac{\partial}{\partial y_4}\left[\lambda_s y_4 + C y_3^3 + \gamma\left(y_3 - y_1\right)\right],\ \mathcal{L}_6 = \frac{W_{02}}{2}\frac{\partial^2}{\partial y_4^2}.$$

To simulate this Fokker-Planck equation, we use the following numerical values of the parameters (according to [7]) :

$$\begin{cases} k_1 = 4000N.m^{-1}\ , \\ \lambda_1 = 100N.s.m^{-1}\ , \\ M = 4000Kg\ , \\ \gamma = 1000N.m^{-1}\ , \\ m = 4000Kg\ , \\ \lambda_s = 300N.s.m^{-1}\ , \\ C = 600N.m^{-3}\ . \end{cases} \tag{14}$$

Moreover, we choose the following parameters of the simulation : $W_0 = 10$, $\Delta t = 0.01\pi$, $N = 20$, $L_1 = L_2 = L_3 = L_4 = 6.0$.
In order to check the accuracy of the solution obtained through numerical integration of the Fokker-Planck equation, we perform Monte Carlo simulations using the fact that the system of dynamical equations (9) can also be written as a system of two stochastic differential equations. We choose Itô's stochastic calculus, so :

$$\begin{cases} dX_1(t) = X_2(t)dt \\ dX_2(t) = \left[-\dfrac{\lambda_1}{M}X_2(t) - \dfrac{k_1}{M}X_1(t) - \dfrac{\gamma}{M}\left(X_1(t) - X_3(t)\right)\right]dt + dW_1(t) \\ dX_3(t) = X_4(t)dt \\ dX_4(t) = \left[-\dfrac{\lambda_s}{m}X_4(t) - \dfrac{c}{m}X_3^3(t) - \dfrac{\gamma}{m}\left(X_3(t) - X_1(t)\right)\right]dt + dW_2(t)\ , \end{cases} \tag{15}$$

with $\left\{\begin{array}{l} X_1(0) = X_{10} \\ X_2(0) = X_{20} \\ X_3(0) = X_{30} \\ X_4(0) = X_{40} \end{array}\right\}$, $0 \leq t \leq T$ ([9], [10]).

By setting $X(t) = \begin{Bmatrix} X_1(t) \\ X_2(t) \\ X_3(t) \\ X_4(t) \end{Bmatrix}$, $f(X) = \begin{Bmatrix} X_2(t) \\ -\frac{\lambda_1}{M}X_2(t) - \frac{k_1}{M}X_1(t) - \frac{\gamma}{M}\left(X_1(t) - X_3(t)\right) \\ X_4(t) \\ -\frac{\lambda_s}{m}X_4(t) - \frac{c}{m}X_3^3(t) - \frac{\gamma}{m}\left(X_3(t) - X_1(t)\right) \end{Bmatrix}$,

$g(X) = \begin{Bmatrix} 0 \\ 1 \\ 0 \\ 1 \end{Bmatrix}$ and $W = \begin{Bmatrix} 0 \\ W_1(t) \\ 0 \\ W_2(t) \end{Bmatrix}$, we can write equation (15) in the form :

$$dX(t) = f\left(X(t)\right)dt + g\left(X(t)\right).dW(t), \;\; X(0) = X_0, \;\; 0 \leq t \leq T \;\; . \qquad (16)$$

The functions $f(x)$ et $g(x)$ are continuous (and in particular, right-continuous with a limit to the left and lipschiz-continuous), so we can claim ([2], [3], [4], [20]...) the existence and unicity of the solution of (16).

While comparing the moments of the motion calculated through Monte Carlo simulation (simulation of the white noise) and those assessed via the Fokker-Planck probability density function, we observe that they are similar but not equal (see figures 11). It is difficult to know which one of these methods is the most false. Indeed, the Monte Carlo simulation needs many draws and much time before converging.

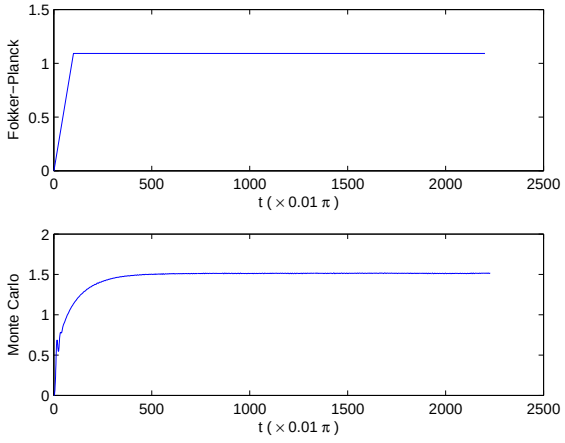

Figure 11. Second moment of the position of the non-linear oscillator, of the system of equation (9), without sollicitation, $W_{01} = W_{02} = 40$ and $\Delta t = 0.01\pi$.

The issue is that the density function is given by arrays belonging to $\mathbb{R}^4$. So to represent the phenomenon of energy pumping, we may calculate marginal

probability densities depending just on two variables. Here we choose to focus on the marginal density of the first oscillator, that of the second one and the marginal density of the two positions.
The Fokker-Planck probability density function of the linear oscillator first presents the gaussian initial condition centered on $(0, \sqrt{2h})$. Then it flattens before taking the shape of the non-normal mode ([27]), as can be seen in figures 12.

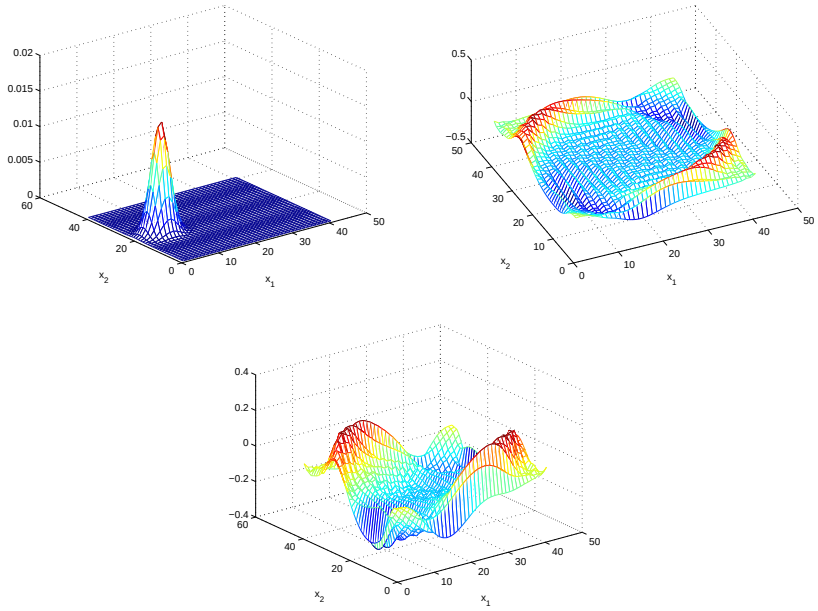

Figure 12. Fokker-Planck probability density function of the first oscillator of equation (9) (the linear one) with parameters of equation (14). The times that are drawn here are $t = 0$, $t = 1000\Delta t$ and $t = 5900\Delta t$ (on the second line), with $\Delta t = 0.001\pi$. Initially, this oscillator is not at rest. But rapidly, its motion stops before spreading upon the track of the non-normal mode.

Now, if we study the probability density function for the second oscillator of the system following equation (9). We first see the initial condition which is gaussian and located in $(0, 0)$. Then the peak disappears and the probability density takes the shape of the non-normal mode (figures 13, page 16).

Finally, the Fokker-Planck probability density function of the positions of both oscillators also proves the phenomenon of energy pumping (figure 14, page 17).

Thus, in 2DOF systems, the deterministic aspects of energy pumping can be meet in this probabilistic study. So, the non-normal modes can be seen if we represent the position of the maximum of probability along time (figure 15, page 17).

These simulations have been made with 41 nodes of the mesh in every di-

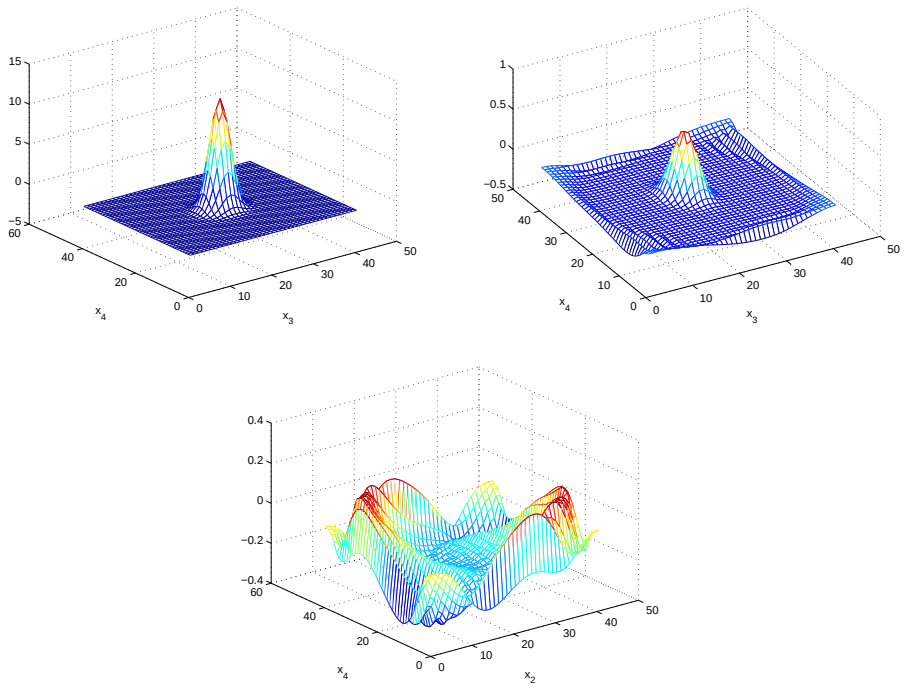

Figure 13. Fokker-Planck probability density function of the system of equation (9) with parameters of equation (14). The times that are drawn here are $t = 0$, $t = 200\Delta t$ and $t = 5900\Delta t$ (on the second line), with $\Delta t = 0.001\pi$. This non-linear oscillator is initially at rest. Then rapidly, it moves and forms the non-normal mode.

rection. In these calculations which work on matrices belonging to $\mathbb{R}^4$, it is possible to decrease the step in space until having 104 nodes of the mesh per direction. But the time of calculation incresases then exponentially.
Moreover, the domain of study chosen here is $L_1 = L_2 = L_3 = L_4 = 6$. Indeed, it seems sufficiently large to take into account of all the dynamics of the system. It could be determined by a deterministic study.

4 Conclusion

In this article, after having written the Fokker-Planck equation in the general case, we proposed a way to resolve it by means of the finite difference method . Then we proved this calculation to be correct and accurate for one DOF systems by comparing it with the analytical solution of a specific case. Finally we studied the motion of some systems : a Duffing-like oscillator whose equilibrium points and strange attractors have so been revealed, a system with Coulomb friction and a two-degree-of-freedom system taking place to energy pumping.
Thus we claim that this method is acceptable for investigating non-linear dynamics of one DOF systems in real noisy environment. For two DOF, it can

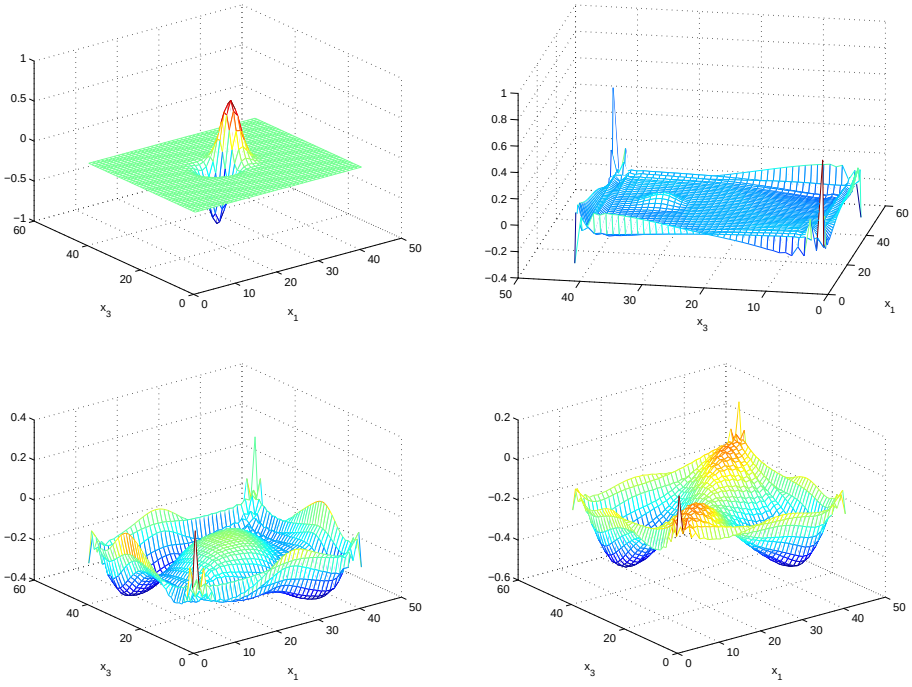

Figure 14. Fokker-Planck probability density function of the positions x and y of the system of equation (9) with parameters of equation (14). The times that are pictured are $t = 0$ $t = 200\Delta t$, $t = 500\Delta t$ and $t = 5900\Delta t$, with $\Delta t = 0.001\pi$.

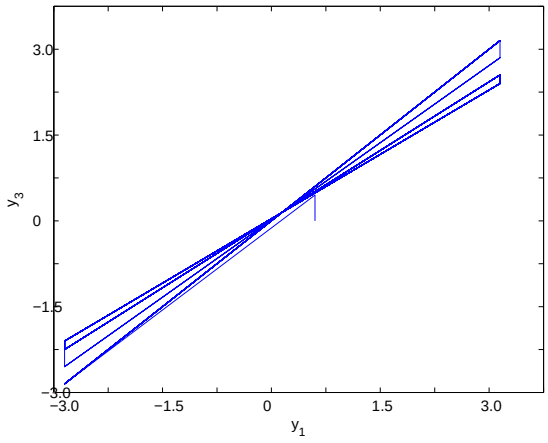

Figure 15. Maximum in $x(= y_1)$ and $y(= y_3)$ of the Fokker-Planck probability density function along time. This probabilistic result is quite the same as the deterministic one (figure 10). The only difference is that in this case, the phenomenon of energy pumping is not finished. This is probably due to the white noise which is always present.

be used in order to obtain qualitative information. Indeed, the exact error cannot be calculated and the simulation is time-consuming and limited (for an ordinary computer). But it may be quite efficient way to test robustness of the energy pumping phenomenon under white noise that may stand for a random forcing (e.g. earthquake) or the intrinsic parameters of the systems that may not be known precisely (e.g. for a building).

References

[1] O. Dessombz, F. Thouverez, J.-P. Laîne, and L. Jézéquel. Analysis of mechanical systems using interval computations applied to finite element methods. *Journal of Sound and Vibration*, 239(5):949–968, 2001.

[2] C. Doléans-Dade. Existence and unicity of solutions of stochastic differential equations. *Z. für Wahrscheinlichkeitstheorie und Verw. Gebiete*, 36(2):93–102, 1976.

[3] C. Doléans-Dade and P.-A. Meyer. Equations différentielles stochastiques. In Irma, editor, *Séminaire de probabilités*, volume 11, pages 376–382, Strasbourg, 1977. Springer-Verlag.

[4] H. Doss and E. Lenglart. Sur l'existence, l'unicité et le comportement asymptotique des solutions d'équations différentielles stochastiques. *Annales de l'I.H.P., section B*, 14(2):189–214, 1978.

[5] O.V. Gendelman and C.H. Lamarque. Dynamics of linear oscillator coupled to strongly nonlinear attachment with multiple states of equilibrium. *Chaos, Solitons and Fractals*, 24(2):501–509, 2005.

[6] R.G. Ghanem and P.D. Spanos. *Stochastic finite elements: A Spectral Approach*. Springer-Verlag, New York, 1991.

[7] E. Gourdon and C.H. Lamarque. Energy pumping for a larger span of energy. *Journal of Sound and Vibration*, 285(3):711–720, 2005.

[8] E. Gourdon and C.H. Lamarque. Energy pumping with various nonlinear structures: Numerical evidences. *Nonlinear Dynamics*, 40(3):281–307, 2005.

[9] D.J. Higham. An algorithmic introduction to numerical simulation of stochastic differential equations. *Society for Industrial and Applied Mathematics*, 43(3):525–546, 2001.

[10] P.E. Kloeden and E Platen. *Numerical Solution of Stochastic Differential Equations*. Springer Verlag, New York, 3rd edition, 1992.

[11] I. Kourakis and A. Grecos. Plasma diffusion and relaxation in a magnetic field. *Communications in Nonlinear Science and Numerical Simulation Chaotic transport and compexity in classical and quantum dynamics*, 8(3-4):547–551, 2003.

[12] A Kunert and F. Pfeiffer. Description of chaotic motion by an invariant probability. *Nonlinear Dynamics*, 2(4):291–304, 1991.

[13] C.-H. Lamarque and J. Bastien. Numerical study of a forced pendulum with friction. *Nonlinear Dynamics*, 23(4):335–352, 2000.

[14] W. Lohmiller and J.-J. E. Slotine. On contraction analysis for non-linear systems. *Automatica*, 34(6):683–696, 1998.

[15] B. R. Mace, K. Worden, and G. Manson. Uncertainty in structural dynamics. *Journal of Sound and Vibration Uncertainty in structural dynamics*, 288(3):423–429, 2005.

[16] J.-M. Malasoma. *Dynamique complexe d'un système à attracteurs multiples.* Phd thesis, Ecole Centrale de Lyon, 1994.

[17] P. S. Neelakanta, S. T. Abusalah, D. F. De Groff, and J. C. Park. Fuzzy nonlinear activity and dynamics of fuzzy uncertainty in the neural complex. *Neurocomputing*, 20(1-3):123–153, 1998.

[18] V.I. Oseledec. A multiplicative ergodic theorem: Lyapunov characteristic numbers for dynamical systems. *Trans. Moscow Math. Society*, 19:197–231, 1968.

[19] W.H. Press, B.P. Flannery, S.A. Teukolsky, and W.T. Vetterling. *Numerical Recipes in C : the Art of Scientific Computing.* Cambridge University Press, Cambridge, 1992.

[20] Ph. E. Protter. On the existence, uniqueness, convergence and explosions of solutions of systems of stochastic integral equations. *Annals of Probability*, 5(2):243–261, 1977.

[21] H. Risken. *The Fokker-Planck equation. Methods of solution and applications*, volume Springer Series in Synergetics. Springer-Verlag, Berlin, second edition edition, 1989.

[22] G. I. Schueller. A state-of-the-art report on computational stochastic mechanics. *Probabilistic Engineering Mechanics A State-of-the-Art Report on Computational Stochastic Mechanics*, 12(4):197–321, 1997.

[23] J. J. E. Slotine and W. Lohmiller. Modularity, evolution, and the binding problem: a view from stability theory. *Neural Networks*, 14(2):137–145, 2001.

[24] C. Soize. Random matrix theory for modeling uncertainties in computational mechanics. *Computer Methods in Applied Mechanics and Engineering Special Issue on Computational Methods in Stochastic Mechanics and Reliability Analysis*, 194(12-16):1333–1366, 2005.

[25] S. Tsakirtzis, G. Kerschen, P. N. Panagopoulos, and A. F. Vakakis. Multi-frequency nonlinear energy transfer from linear oscillators to mdof essentially nonlinear attachments. *Journal of Sound and Vibration*, 285(1-2):483–490, 2005.

[26] Gazanfer Unal and Jian-Qiao Sun. New exact solutions to the fokker-planck-kolmogorov equation. *Communications in Nonlinear Science and Numerical Simulation*, In Press, Corrected Proof, 2007.

[27] A. F. Vakakis. Non-linear normal modes (nnms) and their applications in vibration theory : an overview. *Mechanical Systems and Signal Processing*, 11(1):3–22, 1997.

[28] A. F. Vakakis, L. I. Manevitch, O. Gendelman, and L. Bergman. Dynamics of linear discrete systems connected to local, essentially non-linear attachments. *Journal of Sound and Vibration*, 264(3):559–577, 2003.

[29] M. P. Zorzano, H. Mais, and L. Vazquez. Numerical solution for fokker-planck equations in accelerators. *Physica D: Nonlinear Phenomena Proceedings of the Conference on Fluctuations, Nonlinearity and Disorder in Condensed Matter and Biological Physics*, 113(2-4):379–381, 1998.

[30] M.-P. Zorzano, A.M. Mancho, and L. Vazquez. Numerical integration of the discrete-ordinate radiative transfer equation in strongly non-homogeneous media. *Applied Mathematics and Computation*, 164(1):263–274, 2005.

[31] M.P. Zorzano, H. Mais, and L. Vazquez. Numerical solution of two dimensional fokker–planck equations. *Applied Mathematics and Computation*, 98(2-3):109–117, 1999.